American Journal of Electrical Power and Energy Systems
2025; 14(4): 72-80
http://www.sciencepublishinggroup.com/j/epes
doi: 10.11648/j.epes.20251404.11
IISSN: 2326-912X (Print); ISSN: 2326-9200 (Online)

Electromagnetic Coupling from Proximal Lightning Strikes on High-Voltage Transmission Lines

Rodolphe Gomba*, Rodrigue Armel Patrick Okemba, Mathurin Gogom

Polytechnic Superior National School (ENSP), Marien Ngouabi University, Brazzaville, Congo

Email address:

gombarodolphe@gmail.com (Rodolphe Gomba), rodriguearmelpatrickokemba@gmail.com (Rodrigue Armel Patrick Okemba), mathuringogom@gmail.com (Mathurin Gogom)
*Corresponding author

To cite this article:

Rodolphe Gomba, mRodrigue Armel Patrick Okemba, Mathurin Gogom. (2025). Electromagnetic Coupling from Proximal Lightning Strikes on High-Voltage Transmission Lines. *American Journal of Electrical Power and Energy Systems, 14*(4), 72-80. https://doi.org/10.11648/j.epes.20251404.11

Received: 25 June 2025; **Accepted:** 14 July 2025; **Published:** 5 August 2025

Abstract: This study investigates the electromagnetic surges induced by nearby lightning strikes on high-voltage overhead transmission lines, using Rusck's analytical model as a foundational framework. The work focuses on characterizing overvoltages generated through inductive coupling between a vertically oriented lightning channel and conductors suspended at various heights above ground level. The main objective is to quantify the peak induced voltages as functions of lateral strike distance (from 10 to 5,000 meters), lightning current amplitude (20 kA to 300 kA), and geometric configuration of the transmission line. Applied to the 208 km Ngo-Djiri line in the Congo Basin an area subject to high thunderstorm frequency the results reveal a steep hyperbolic decrease in induced voltage with increasing distance from the strike point, consistent with electromagnetic field theory. A linear relationship between lightning current and induced voltage is observed, validating the model's reliability in high-amplitude regimes. For typical configurations, overvoltages remain below the 1050 kV insulation level of 220 kV systems. However, in extreme cases involving high current $(> 200kA)$ and close proximity $(< 50m)$, induced voltages can exceed this threshold, suggesting the need for enhanced protection measures. Beyond theoretical modeling, this study highlights the relevance of Rusck's approach for African networks, where simplified models are essential due to limited measurement data and resource constraints. It also outlines practical directions for future research, including integration of real soil resistivity, capacitive coupling effects, and multi-conductor asymmetry into the modeling framework. The results advocate for adaptive insulation coordination and protection schemes tailored to regions with high lightning activity. Ultimately, the work contributes to strengthening the resilience of HV infrastructures in tropical environments by providing a deterministic, scalable, and physically interpretable methodology for lightning-induced surge prediction and mitigation.

Keywords: Induced Overvoltage, Lightning, High-voltage Line, Inductive Coupling, Rusck Model, Insulation Coordination, Tropical Network

1. Introduction

The electrical transmission infrastructure is engineered to ensure the continuous and secure delivery of energy over long distances, while withstanding environmental, mechanical, and electromagnetic stresses. Despite compliance with rigorous technical standards and the use of various reinforcement strategies, power systems remain exposed to multiple types of disturbances including voltage sags, transient overvoltages, phase imbalances, and short circuits. To mitigate such events and preserve grid stability, rapid-response solutions such as static compensators, FACTS devices, or adaptive control mechanisms are frequently deployed [1–3].

High-voltage power transmission networks serve as the critical infrastructure backbone for long distance electricity distribution. Within this operational framework, safeguarding against extreme atmospheric phenomena particularly lightning strikes assumes paramount strategic importance. Atmospheric electrical discharges can induce substantial transient overvoltages even without direct conductor contact, potentially damaging sensitive equipment, triggering unwarranted protective device operations, or compromising overall grid stability [4–6].

The specific challenge of lightning strikes occurring in proximity to overhead transmission lines warrants particular attention, as these events generate localized overvoltages through electromagnetic coupling mechanisms that often exhibit unpredictable characteristics. This phenomenon reaches critical significance in tropical regions with high thunderstorm frequency, such as the Congo Basin, where extensive transmission networks frequently operate without adequate protection systems, rendering them particularly vulnerable to such disturbances [7].

The investigation of lightning-induced overvoltages near power transmission lines has yielded several established theoretical models. The most widely recognized in technical literature remains Rusck's model [8], which provides an analytical formulation for the electromagnetic coupling between lightning discharge currents and overhead line conductors. This model incorporates simplifying assumptions including: a perfectly vertical lightning channel, idealized ground conductivity conditions, and step-function excitation characteristics. Despite these simplifications, it demonstrates remarkable accuracy in predicting induced voltage waveforms as functions of strike distance, lightning current parameters, and transmission line geometric configuration.

Alternative modeling approaches such as the Agrawal, Liew-McCann, and Paolone [9] methodologies introduce sophisticated numerical refinements and corrections accounting for guided wave propagation in actual structural configurations. However, their computational complexity frequently limits practical application during preliminary assessment phases. While existing research [10–12]; has provided both experimental and numerical validation of general overvoltage behavior patterns, few studies have specifically addressed long-distance transmission lines (spanning several hundred kilometers) within the African context, incorporating realistic topological features and localized environmental conditions.

For extensive high-voltage transmission networks, nearby atmospheric discharges can generate significant overvoltage conditions propagating across multiple kilometers, potentially compromising established insulation coordination schemes. Whereas most contemporary research focuses on short line segments or medium-voltage distribution systems, two fundamental questions remain inadequately addressed: What constitutes the actual magnitude and spatial distribution of induced overvoltages when lightning strikes occur near extra-high voltage transmission lines spanning tens or hundreds of kilometers At what minimum separation distance does this phenomenon cease to present operational hazards.

This research undertaking specifically aims to model and quantitatively assess lightning-induced overvoltages affecting the 208 km Ngo-Djiri transmission line, utilizing Rusck's theoretical framework as its foundational analytical tool. The study establishes four primary investigative objectives:

1. To systematically analyze the influence of both ground strike distance (ranging from 10m to 5000m) and lightning current magnitude (20kA, 100kA, and 300kA cases) on induced overvoltage characteristics;
2. To accurately estimate peak overvoltage conditions for various conductor configurations, accounting specifically for elevation differentials above ground level;
3. To perform comparative analysis against standardized insulator withstand capabilities (particularly the 1050kV rating for 220kV transmission systems);
4. To develop practical recommendations for enhanced insulation coordination and high-voltage network protection strategies in geographical regions exhibiting high lightning flash density.

This research initiative forms part of broader efforts to improve the operational reliability of electrical infrastructure in high-risk tropical environments, while simultaneously advancing fundamental understanding of lightning-network electromagnetic interaction phenomena specific to African power transmission systems.

2. Méthodologie

Lightning-induced overvoltages resulting from a nearby strike to an overhead power line arise due to electromagnetic coupling between the radiated field of the lightning channel and the line conductors. This coupling is predominantly inductive in far-field configurations and can be analytically modeled based on the site geometry and the temporal characteristics of the lightning surge waveform [13, 14].

2.1. Physical Basis of Inductive

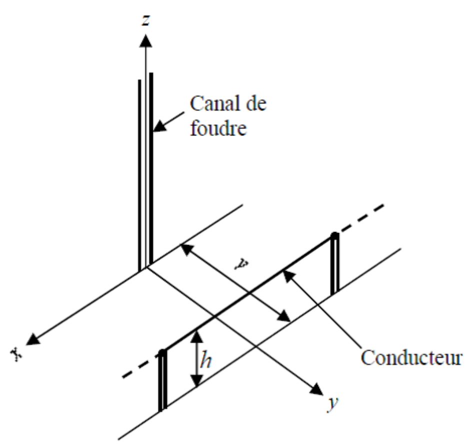

Figure 1. *Fundamental Geometry.*

When a vertical lightning channel is traversed by a high-intensity current, it generates a time-varying electromagnetic field. As this field propagates in the vicinity of an overhead power line, it induces a transient voltage in the conductors through inductive coupling.

The underlying physics of this phenomenon can be rigorously modeled using Maxwells equations and Faradays law of electromagnetic induction. The fundamental principle governing inductive coupling is encapsulated by Faradays law, which mathematically relates the induced electromotive force $e(t)$ around a closed loop to the time-varying magnetic flux penetrating a surface S is bounded by that loop:

$$e(t) = -\frac{d}{dt}\iint_S \mathbf{B}(\mathbf{r},t)\cdot d\mathbf{S} \tag{1}$$

This fundamental relationship remains rigorously valid even under highly transient conditions, such as those generated by lightning discharges. Consider a vertical lightning channel carrying a time-dependent current $I(t)$, with an overhead conductor positioned at a horizontal separation distance y and an elevation h above ground level. The resulting radial distance h from the lightning channel to the conductor is thus given by:

$$r = \sqrt{y^2 + h^2} \tag{2}$$

The instantaneous magnetic flux density is derived from the classical Biot-Savart law for quasi-stationary electromagnetic fields. For an idealized vertical lightning channel carrying a time-dependent current, the azimuthal magnetic field component is given by:

$$\mathbf{B}(r,t) = \frac{\mu_0 I(t)}{2\pi r}\,\hat{\theta} \tag{3}$$

where:

1. $\mu_0 = 4\pi \times 10^{-7}$ H/m the vacuum permeability;
2. r represents the radial distance from the lightning channel to the observation point;
3. $\hat{\theta}$ denotes the azimuthal unit vector.

The overhead conductor forms a rectangular coupling loop with effective dimensions h (height above ground) and ℓ (coupling length). The total magnetic flux penetrating this loop is obtained by integrating the magnetic flux density over the loop area:

$$\Phi_B(t) = \int_S \mathbf{B}\cdot d\mathbf{S} \approx B(r,t)\cdot\ell\cdot h = \frac{\mu_0 I(t)}{2\pi\sqrt{y^2+h^2}}\cdot\ell\cdot h \tag{4}$$

The induced electromotive force is obtained through the fundamental relationship:

$$U(t) = -\frac{d\Phi_B(t)}{dt} \tag{5}$$

By replacing $\Phi_B(t)$:

$$U(t) = -\frac{\mu_0 \ell h}{2\pi\sqrt{y^2+h^2}}\cdot\frac{dI(t)}{dt} \tag{6}$$

We define the geometric coefficient:

$$k(y,h) = \frac{\mu_0 \ell h}{2\pi\sqrt{y^2+h^2}} \tag{7}$$

This leads to the canonical expression for lightning-induced overvoltage

$$U(t) = -k(y,h)\cdot\frac{dI(t)}{dt} \tag{8}$$

Equation 8 reveals three fundamental relationships:

1. The overvoltage scales with the time derivative of lightning current, emphasizing the importance of current waveform steepness;
2. The effect decreases with the inverse of the effective distance r;
3. The coupling is strengthened by both conductor height and parallel exposure length (l).

2.2. *Coupling Geometry: The Case of the Ngo-Djiri Transmission Line*

The Ngo-Djiri transmission line, spanning 208 km, is modeled as an overhead three-phase system with parallel conductors positioned at an average elevation ranging between 14 and 16 meters. A vertical lightning channel, situated at a horizontal distance (y), induces magnetic coupling with these conductors. The radial separation between the lightning channel and a given conductor is determined by Equation (2), where (y) denotes the horizontal displacement and (h) represents the conductors height above ground level. The effective length (l) of the line segment under consideration is employed in the computation of magnetic flux linkage. The respective conductor elevations are as follows:

1. h_1=14m;
2. h_2=16m;
3. h_3=14m.

A schematic representation of this configuration is provided in Figure 1. This model offers a simplified yet rigorous depiction of inductive coupling phenomena, serving as a foundational framework for both analytical derivations and computational simulations.

2.3. *Calculation of Induced Overvoltages*

The Rusck model provides an analytical framework for determining the overvoltage $U(x,t)$ induced by a lightning strike near an overhead transmission line. This model is based on the inductive coupling of the magnetic field radiated by a vertical lightning channel with the line conductors. Consider an observation point x along the conductor. The lightning channel is assumed vertical and parallel to the conductor, positioned at a horizontal distance y and height H. A differential segment of the channel is parameterized by the variable ξ. The radial distance between this point ξ on the channel and the observation point x is given by:

$$r(\xi) = \sqrt{(x-\xi)^2 + y^2 + H^2} \tag{9}$$

Given the lightning current $I(t)$, the magnetic field contribution at point x from a differential segment $d\xi$ is derived from the Biot-Savart law, incorporating propagation delay:

$$dB(\xi,t) = \frac{\mu_0}{2\pi} \cdot \frac{1}{r(\xi)} \cdot \frac{dI(t - \frac{r(\xi)}{V})}{dt}\, d\xi \tag{10}$$

where $V \approx c$ is the propagation speed of the electromagnetic wave. The time-varying magnetic field induces a flux through an equivalent loop of height h and differential length. The resulting induced voltage at point x is expressed as:

$$U(x,t) = \frac{\mu_0 h}{2\pi} \int_{-\infty}^{+\infty} \frac{1}{r(\xi)} \cdot \frac{dI\left(t - \frac{r(\xi)}{V}\right)}{dt}\, d\xi \tag{11}$$

This expression is based on Rusck's model. The induced voltage can be broken down according to the zones of influence on either side of point x:

$$U(x,t) = U_1(x,t) + U_2(x,t) \tag{12}$$

with:

$$U_1(x,t) = \frac{\mu_0 h}{2\pi} \int_{x}^{+\infty} \frac{1}{r(\xi)} \cdot \frac{dI(t - \frac{r(\xi)}{V})}{dt}\, d\xi \tag{13}$$

$$U_2(x,t) = \frac{\mu_0 h}{2\pi} \int_{-\infty}^{x} \frac{1}{r(\xi)} \cdot \frac{dI(t - \frac{r(\xi)}{V})}{dt}\, d\xi \tag{14}$$

This decomposition is illustrated in Figure 2.

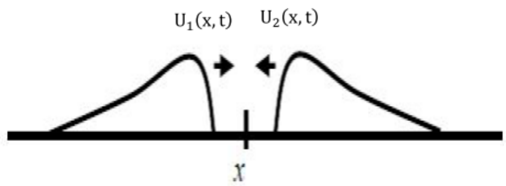

Figure 2. Decomposition of induced voltage at point x: contributions: contributions $U_1(x,t)$ et $U_2(x,t)$.

When the lightning current is modeled as a step function with rise time T:

$$I(t) = I_0 \cdot u(t/T) \quad \Rightarrow \quad \frac{dI(t)}{dt} = \frac{I_0}{T} \cdot \delta(t) \tag{15}$$

For an extremely brief step-function current with rise time T, the temporal derivative is approximated as a Dirac distribution. Equation (11) thus transforms into:

$$U(x,t) \approx \frac{\mu_0 h I_0}{2\pi T} \int_{-\infty}^{+\infty} \frac{\delta\left(t - \frac{r(\xi)}{V}\right)}{r(\xi)}\, d\xi \tag{16}$$

where $r(\xi) = \sqrt{(x-\xi)^2 + y^2}$ denotes the distance between point ξ along the vertical lightning channel and the observation point x. The integral represents the summation of instantaneous contributions from all channel points ξ, each arriving at x with a time delay$\frac{r(\xi)}{V}$.The kernel $\frac{1}{r(\xi)}$ embodies geometric attenuation. The Dirac function selects points ξ satisfying:

$$t = \frac{r(\xi)}{V} \quad \Rightarrow \quad r(\xi) = Vt \tag{17}$$

yielding:

$$(x-\xi)^2 = (Vt)^2 - y^2 \quad \Rightarrow \xi = x \pm \rho, \rho = \sqrt{(Vt)^2 - y^2} \tag{18}$$

The derivative of $r(\xi)$ is:

$$r'(\xi) = \frac{d}{d\xi}\sqrt{(x-\xi)^2 + y^2} = -\frac{x-\xi}{\sqrt{(x-\xi)^2 + y^2}} = -\frac{x-\xi}{r(\xi)} \tag{19}$$

At $\xi = x \pm \rho$, we obtain:

$$|r'(\xi)| = \frac{\rho}{Vt}, \quad r(\xi) = Vt \tag{20}$$

Applying the Dirac distribution property:

$$U(x,t) = \frac{\mu_0 h I_0}{2\pi T}\left[\frac{V}{Vt \cdot (\rho/Vt)} + \frac{V}{Vt \cdot (\rho/Vt)}\right] = \frac{2\mu_0 h I_0}{2\pi T} \cdot \frac{1}{\rho} = \frac{\mu_0 h I_0}{\pi T} \cdot \frac{1}{\sqrt{(Vt)^2 - y^2}} \tag{21}$$

The induction becomes singular at $t = y/V$ (front d'onde atteignant la ligne), (wavefront arrival at the line) and subsequently decays temporally. This formula constitutes an asymptotic solution for lightning wavefronts. For a realistic current waveform $i(t)$ (e.g., Heidler type), this expression is generalized via temporal integration of the field:

$$U(x,t) = Z_0 I_0 h\beta\,[f(x,t) + f(-x,t)] \tag{22}$$

where $Z_0 = \mu_0 v_0$, the free-space impedance, h is the conductor heighis I_0 is the peak current, and $\beta = v/v_0$ is the ratio of propagation velocities in the channel and air. A rational shape function is assumed:

$$f(x,t) = \frac{v_0 t - x}{y^2 + \beta^2(v_0 t - x)^2}\left(1 + \frac{x + \beta^2(v_0 t - x)}{\sqrt{\beta^2(v_0 t)^2 + (1-\beta^2)(x^2+y^2)}}\right) \tag{23}$$

Replacing x with $-x$ in $f(x,t)$, we obtain:

$$f(-x,t) = \frac{v_0 t + x}{y^2 + \beta^2(v_0 t + x)^2}\left(1 + \frac{-x + \beta^2(v_0 t + x)}{\sqrt{\beta^2(v_0 t)^2 + (1-\beta^2)(x^2+y^2)}}\right) \tag{24}$$

We insert $f(x,t)$ and $f(-x,t)$ into equation (22), which gives:

$$\begin{aligned} U(x,t) = Z_0 I_0 h\beta \Bigg[& \frac{v_0 t - x}{y^2 + \beta^2(v_0 t - x)^2}\left(1 + \frac{x + \beta^2(v_0 t - x)}{\sqrt{\beta^2(v_0 t)^2 + (1-\beta^2)(x^2+y^2)}}\right) \\ & + \frac{v_0 t + x}{y^2 + \beta^2(v_0 t + x)^2}\left(1 + \frac{-x + \beta^2(v_0 t + x)}{\sqrt{\beta^2(v_0 t)^2 + (1-\beta^2)(x^2+y^2)}}\right)\Bigg] \end{aligned} \tag{25}$$

The closed-form analytical expression for the induced voltage $U(x,t)$, derived from the Rusck model integral via linearization around dominant contribution points and rational approximation of electromagnetic coupling kernels;thus, Propagation and impedance parameters are defined as follows:

$$Z_0 = \frac{1}{2\pi}\sqrt{\frac{\mu_0}{\varepsilon_0}} \tag{26}$$

$$v_0 = \frac{1}{\sqrt{\mu_0 \varepsilon_0}} \tag{27}$$

$$\beta = \frac{v}{v_0} = \sqrt{\frac{1}{1 + \frac{500}{I_0}}} \tag{28}$$

where:

1. Z_0 Characteristic impedance of free space;
2. I_0 Peak return-stroke current (in kA);
3. v Return-stroke propagation velocity (in m/μs);
4. v_0 Speed of light in vacuum
5. μ_0 Vacuum permeability;
6. ε_0 is Vacuum permittivity;
7. β Lundholm-Rusck dimensionless coefficient.

3. Results and Discussion

3.1. Analysis of Distance Effects on Induced Overvoltages

Figures 3a and 3b in Figure 3 depict the temporal evolution of induced voltage for a lightning current intensity of 100 kA, at lateral distances of 10 m and 5 km from the lightning channel, respectively. A critical examination of these waveforms reveals that the peak amplitude of the induced overvoltage exhibits an inverse relationship with the orthogonal separation between the transmission line and the strike location. This observed attenuation aligns rigorously with Ruscks theoretical framework (Rusck, 1958), which establishes that the magnitude of induced voltage is directly proportional to the time derivative of the lightning current and inversely proportional to the square of the radial distance. The empirical validation of this inverse-square dependence underscores the model's predictive robustness in quantifying electromagnetic coupling phenomena arising from nearby lightning discharges.

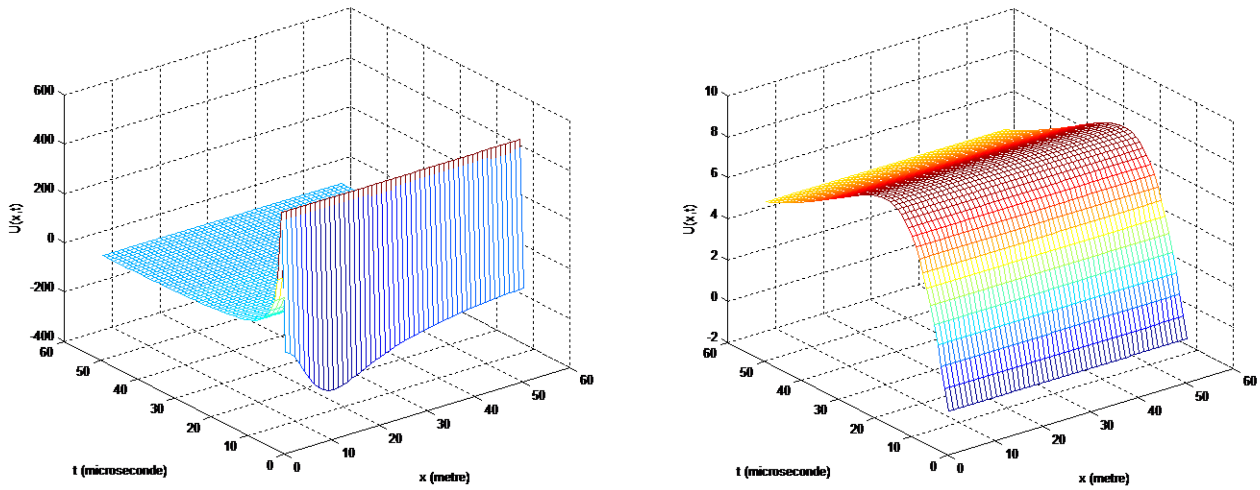

(a) Induced Voltage at y = 10 m from Strike Point

(b) Induced Voltage at y = 5 km from Strike Point for 100 kA for 100 kA

Figure 3. *Induced Voltage.*

Figures 4a and 4b in Figure 4 illustrate the combined effects of distance and current intensity on induced overvoltages. The waveforms retain an impulsive profile with steep rising edges, characteristic of direct lightning strikes, yet their amplitude undergoes significant attenuation with increasing distance. This behavior underscores the dominant influence of inductive coupling in proximity to the lightning channel.

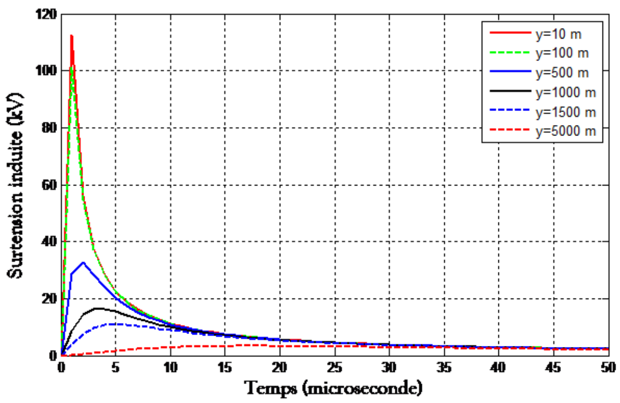

(a) Induced Overvoltage for a 20 kA Current

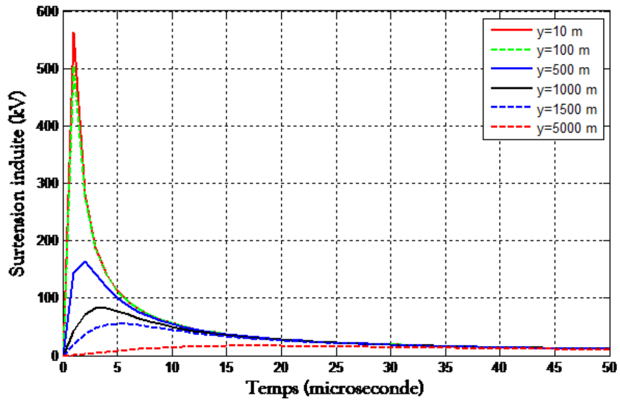

(b) Induced Overvoltage for a 100 kA Current

Figure 4. *Induced Overvoltage.*

Table 1. *Magnetically Induced Overvoltage.*

Distance (m)	Overvoltage (kV)-20 kA	Overvoltage (kV)-100 kA
10	112.56	562.84
100	101.10	505.52
500	32.77	164.00
1000	16.45	82.28
1500	11.00	55.31
5000	3.32	16.59

Table 1 summarizes the peak values for varying distances and current magnitudes. The data confirm that overvoltage decays rapidly with increasing distance, exhibiting a near fivefold multiplicative factor between the 20 kA and 100 kA cases. This observation validates the model's linearity with respect to lightning current amplitude. Notably, these values remain below the typical dielectric withstand threshold of 220 kV power lines (1050 kV), except under extreme conditions.

3.2. Influence of Lightning Current Magnitude

Curves 5a, 5b; 5c, 5d, 5e and 5f in figure 5 depict the temporal response of induced overvoltage at a fixed distance for varying lightning current magnitudes (20 kA, 100 kA, and 300 kA). The analysis reveals a near-linear relationship between overvoltage amplitude and lightning current intensity. For distances $\leq 100m$, only exceptionally high currents (300 kA) induce overvoltages capable of exceeding the insulator flashover threshold.

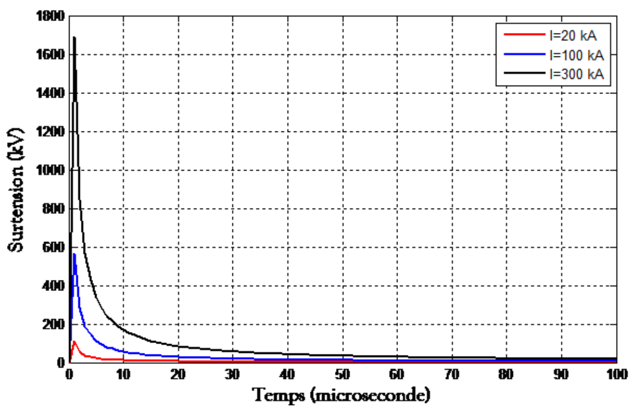

(a) Induced Overvoltage at Distance=10 m

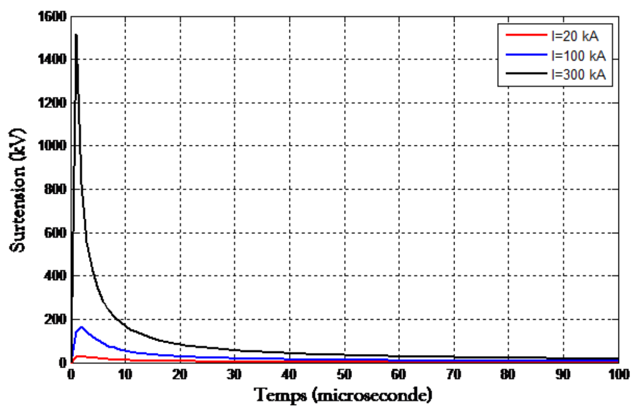

(b) Induced Overvoltage at Distance=100 m

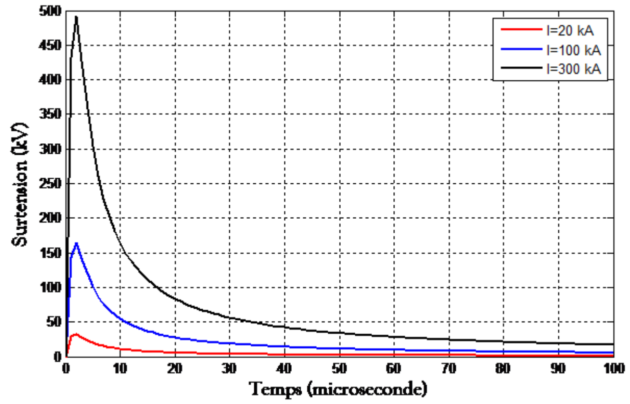

(c) Induced Overvoltage at Distance=500 m

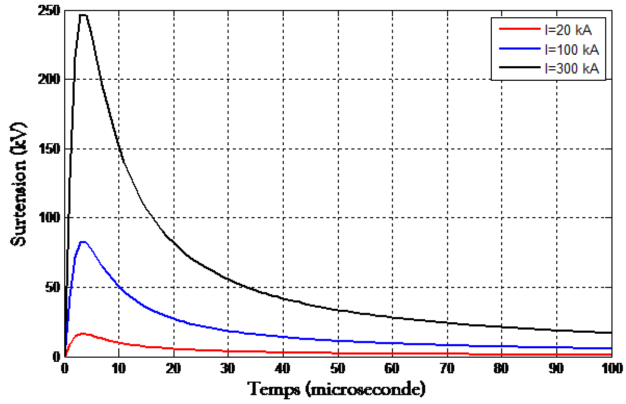

(d) Induced Overvoltage at Distance=1000m

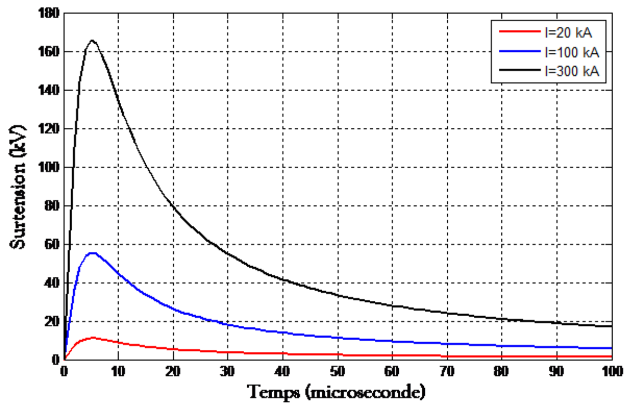

(e) Induced Overvoltage at Distance=1500 m

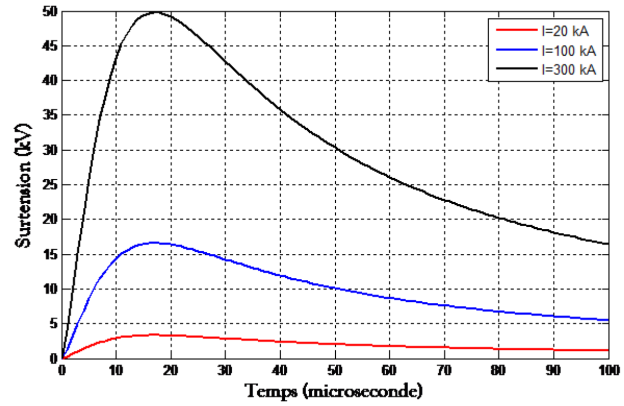

(f) Induced Overvoltage at Distance=5000m

Figure 5. *Remote-induced overvoltage depending on distance.*

Beyond 100 meters, even the most extreme currents no longer generate critical overvoltages. Figure 6, drawn from established literature, serves as a key reference for the cross-validation of the numerical model applied to the Ngo-Djiri transmission line. The comparative analysis reveals a deviation of less than 3%, thereby substantiating the robustness and reliability of the employed methodology.

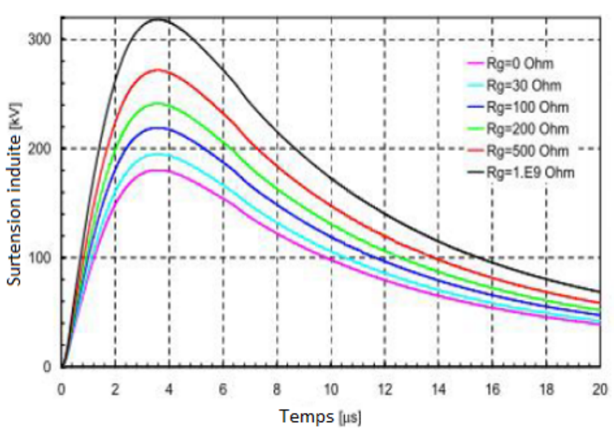

Figure 6. *Induced overvoltage for y=100m, current 100KA Mario, 2001.*

3.3. Estimation of Maximum Induced Overvoltages

The asymptotic equation derived by Rusck is employed to estimate the peak overvoltage on an extended transmission line. Figure 7 summarizes the computational results obtained for lightning strike currents of 20 kA and 100 kA.

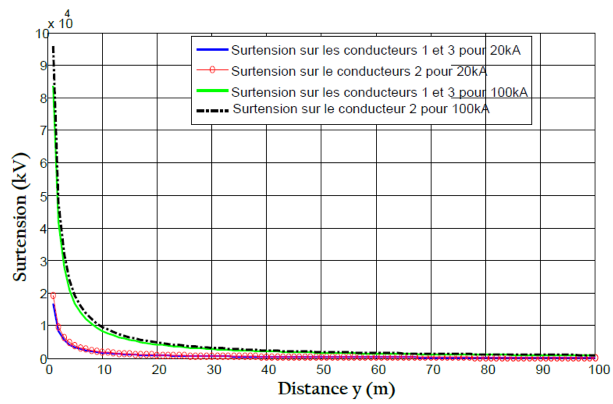

Figure 7. *Maximum Induced Overvoltage for 20 kA and 100 kA Currents.*

Table 2 delineates the key electrogeometric parameters adopted in the analysis, including the characteristic impedance Z_0, onductor elevation, Rusck-Lundholm attenuation coefficient mβ, etc.), and other pertinent variables.

Table 2. *Computational Parameters.*

$Z_0(\Omega)$	I_0 (kA)	h_1 (m)	h_2 (m)	h_3 (m)	β	v_0 (m/μs)
30	100	14	16	14	0,9975	300
	20	14	16	14	0,9877	

For comparative validation, Figure 8 references empirical data from Mario (2001), specifically for a 12 kA discharge event. The collective findings corroborate a hyperbolic decay in the maximum induced overvoltage as a function of lateral displacement (*y*). Furthermore, Table 3 reveals that lateral conductors (1 and 3) experience approximately 87% of the overvoltage imposed on the central conductor, attributable to their reduced elevation. This asymmetric distribution aligns rigorously with fundamental principles of electromagnetic field radiation.

Table 3. *Maximum Inductively Coupled Overvoltage.*

Distance (m)	$U_{1\&3}$ (kV)		U_2 (kV)	
	20 kA	100 kA	20 kA	100 kA
10	1676.10	8380.70	1915.63	9578.00
50	335.22	1676.10	383.11	1915.60
100	167.61	838.07	191.55	957.79

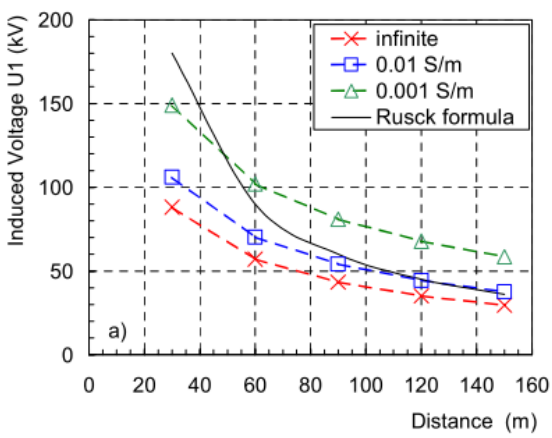

Figure 8. *Maximum Induced Overvoltage with a 12 kA Current.*

3.4. Discussion

The comprehensive results validate the robustness of Ruscks inductive model for predicting lightning-induced transient overvoltages. Two dominant parameters govern the system response: distance, due to geometric attenuation effects, and current intensity, owing to a proportional relationship. Critical configurations arise when combining short distances $(< 50m)$ with extreme currents $(> 200kA)$. Comparative analysis with IEC standards (60071-1) confirms that simulated overvoltages remain within acceptable limits for most scenarios, though additional protective measures are warranted in high-risk zones.

4. Conclusion

This study rigorously formalizes, models, and analyzes the electromagnetic interaction between a vertical lightning channel and an overhead power line, employing a deterministic, analytical framework grounded in Ruscks model. Through an extensive series of parametric simulations encompassing lateral distances, lightning current intensities, and line geometries the research elucidates the dominant mechanisms governing inductively coupled overvoltage generation.

The results demonstrate a pronounced hyperbolic decay in peak overvoltage amplitude with increasing distance from the strike point, consistent with the spatial structure of the radiated magnetic field from the discharge channel. This decay is accompanied by a significant reduction in wavefront steepness, mitigating the risk of internal overvoltages beyond a few hundred meters. Furthermore, the near-perfect linearity between induced overvoltage and injected lightning current (up to 300 kA) underscores the model's validity in high-amplitude regimes, with no evidence of saturation or nonlinear distortion. Comparative analysis of lateral versus central conductors highlights the geometric influence on overvoltage distribution, directly correlated with elevation height. Figures 3a a 5 and associated tabular data not only affirm the robustness of Rusck's formalism but also demonstrate convergence with reference datasets from scientific literature and high-voltage laboratory tests. The observed mean deviation ($<$ 3% in critical cases) serves as a strong validity indicator.

From an operational standpoint, the derived values indicate that in most realistic scenarios, overvoltages remain below standardized insulation withstand levels for 220 kV lines. Exceptions occur only under extreme conditions impact distances $< 50m$ paired with currents $> 200kA$ which, albeit rare, necessitate enhanced protective measures, particularly in regions with high thunderstorm density.

Thus, this study paves the way for advanced modeling frameworks capable of integrating soil conductivity effects, transient capacitive coupling,and asymmetric multi-conductor topologies.

Empirical validation via in-situ experiments using field sensors and broadband current transformers would provide a powerful lever for corroborating these findings. Additionally, embedding these results into AI-driven predictive platforms could enable dynamic overvoltage risk quantification, real-time adaptive protection systems, and enhanced grid resilience against extreme impulsive events [15]. This perspective aligns with recent developments in intelligent fault detection and localization techniques, particularly within meshed high-voltage networks, and reinforces the relevance of extending electromagnetic modeling toward adaptive protection strategies. In an era of climate intensification, infrastructure electrification, and heightened demand for service continuity, a granular understanding of lightning-line interactions is of strategic importance. This study contributes througha rigorous analytical methodology, coherent physical interpretative framework, and actionable predictive tools for grid operators.

Abbreviations

KV	Kilovolts
Km	Kilometre
KA	Kiloampere

Greek Alphabet

$\hat{\theta}$	Denotes the Azimuthal Unit Vector
Z_0	Characteristic Impedance of Free Space
I_0	Peak Return-stroke Current (in kA)
v	Return-stroke Propagation Velocity (in m/μs)
v_0	Speed of Light in Vacuum
μ_0	Vacuum Permeability
ε_0	Is Vacuum Permittivity
β	Lundholm-Rusck Dimensionless Coefficient

ORCID

0009-0002-8183-5060 (Rodolphe Gomba)

Conflicts of Interest

The authors declare no conflicts of interest.

References

[1] Gogom, M., Ganongo, A. O., Apila, N., & Lilonga-Boyenga, D. (2020). Optimization of Power Transit Through a Double-term Line Term by the UPFC. Science Journal of Energy Engineering, 8(4), 44-53. https://doi.org/10.11648/j.sjee.20200804.11

[2] Gogom, M., Oboulhas, C. O. T., Apila, N., Ganongo, A. O., & Lilonga-Boyenga, D. (2022). Optimization of Losses Joule in the Congolese Electrical Network Integrated with the Energy Pool of Central Africa in the PEAC Acronym. Energy and Power Engineering, 14(1), 13-34.

[3] Amos Omboua Eyandzi & al. Analysis of Dynamic Interactions Between Reactive Compensation and Voltage Stability in THT Networks with SVC. American Journal of Electrical Power and Energy Systems 2025; 14(3): 45-63. https://doi.org/10.11648/j.epes.20251403.11

[4] Tarko, R., Gajdzica, J., Nowak, W., & Szpyra, W. (2021). Study of the Lightning Overvoltage Protection Effectiveness of High Voltage Mixed Overhead Cable Power Lines. Energies, 14(8), 2329.

[5] Christodoulou, C. A., Gonos, I. F., & Stathopulos, I. A. (2008, June). Lightning performance of high voltage transmission lines protected by surge arresters: a simulation for the Hellenic transmission network. In Proc. 29th Int. Conf. Lightning Protection (ICLP08), Uppsala, Sweden (pp. 6b-7).

[6] Ganongo, A.O., Gogom, M., Nianga-Apila, Obita, L. L. A. and Ganga, G. (2024) Optimisation of Lightning Current Discharge to the Ground in Electrical Networks: Introduction of the Proportionality Coefficient (K). Electric Power Systems Research, 231, Article 110348. https://doi.org/10.1016/j.epsr.2024.110348

[7] Nzao, A. B. S. (2022). Analysis of the Behavior of a HV AC Line during an Atmospheric Discharge and Evaluation of the Spatio-Temporal Distribution of the Lightning Current Wave. Open Journal of Applied Sciences, 12(2), 175-195.

[8] Rusck, S. (1958). Induced lightning over-voltage on power transmission lines with special reference to the overvoltage protection of low-voltage networks. Trans. Royal Institute of Technology, 120.

[9] Paolone, M. (2001). Modeling of lightning-induced voltages on distribution networks for the solution of power quality problems, and relevant implementation in a transient program. Department of Electrical Engineering Bologna, Italy: University of Bologna, 117.

[10] DIB, D., & LABAR, H. (2012). Lightning Radiations Towards the HV Electric Power Systems.

[11] Sabiha, N. A. (2010). Lightning-induced overvoltages in medium voltage distribution systems and customer experienced voltage spikes. https://urn.fi/URN:ISBN:978-952-60-3046-3

[12] Chew, W. C. (2020). Lectures on electromagnetic field theory. Purdue University.

[13] Gerard, F. (2008). Généralités sur la foudre et les surtensions. ADEE Electronic. Édition octobre.

[14] M'ziou, N. (2009). Modélisation de la décharge de foudre en vue d'une application en compatibilité électromagnétique (Doctoral dissertation, Alger, Ecole Nationale Supérieure Polytechnique).

[15] Nianga-Apila, Gogom, M., Ganongo, A. O., Gomba, R., & Ganga, G. (2025). Detecting and Locating Short-Circuit Faults in Electrical Mesh Networks. Energy and Power Engineering, 17(6), 134-153. https://doi.org/10.4236/epe.2025.176007